View metadata, citation and similar papers at core.ac.uk

brought to you by CORE

provided by Texas A&M Repository

Retinoic acid deficiency alters second heart field formation

Lucile Ryckebusch*, Zengxin Wang†, Nicolas Bertrand*, Song-Chang Lin†, Xuan Chi‡, Robert Schwartz‡, Stéphane Zaffran*§, and Karen Niederreither†§

*Developmental Biology Institute of Marseille-Luminy, Centre National de la Recherche Scientifique Unité Mixte de Recherche 6216, Campus de Luminy Case 907, 13009 Marseille, France; †Departments of Medicine and Molecular and Cellular Biology, Center for Cardiovascular Development, Baylor College of Medicine, One Baylor Plaza, Houston, TX 77030; and ‡Center for Molecular Development and Diseases, Institute of Biosciences and Technology, Texas A&M University, Houston, TX 77030

Communicated by Pierre Chambon, Institut de Génétique et de Biologie Moleculaire et Cellulaire, Strasbourg, France, December 31, 2007 (received for review August 29, 2007)

Retinoic acid (RA), the active derivative of vitamin A, has been implicated in various steps of cardiovascular development. The retinaldehyde dehydrogenase 2 (RALDH2) enzyme catalyzes the second oxidative step in RA biosynthesis and its loss of function creates a severe embryonic RA deficiency. *Raldh2*$^{-/-}$ knockout embryos fail to undergo heart looping and have impaired atrial and sinus venosus development. To understand the mechanism(s) producing these changes, we examined the contribution of the second heart field (SHF) to pharyngeal mesoderm, atria, and outflow tract in *Raldh2*$^{-/-}$ embryos. RA deficiency alters SHF gene expression in two ways. First, *Raldh2*$^{-/-}$ embryos exhibited a posterior expansion of anterior markers of the SHF, including *Tbx1*, *Fgf8*, and the *Mlc1v-nlacZ-24*/*Fgf10* reporter transgene as well as of *Islet1*. This occurred at early somite stages, when cardiac defects became irreversible in an avian vitamin A-deficiency model, indicating that endogenous RA is required to restrict the SHF posteriorly. Explant studies showed that this expanded progenitor population cannot differentiate properly. Second, RA up-regulated cardiac *Bmp* expression levels at the looping stage. The contribution of the SHF to both inflow and outflow poles was perturbed under RA deficiency, creating a disorganization of the heart tube. We also investigated genetic cross-talk between Nkx2.5 and RA signaling by generating double mutant mice. Strikingly, *Nkx2.5* deficiency was able to rescue molecular defects in the posterior region of the *Raldh2*$^{-/-}$ mutant heart, in a gene dosage-dependent manner.

retinoids | retinaldehyde dehydrogenase 2 | heart development | Nkx2.5 | FGF8

Cardiogenesis requires specification, proliferation, differentiation, and migration of cell populations from diverse sites. Retinoic acid (RA), the active derivative of vitamin A, by acting as a diffusible activator of nuclear receptors, critically regulates a variety of steps and stages of cardiovascular development (1). Various animal models have been used to examine RA-dependent heart development, including knockout mice deficient in retinaldehyde dehydrogenase 2 (RALDH2), which catalyzes the second oxidative step in RA biosynthesis. *Raldh2*$^{-/-}$ mutants exhibit a severe deficiency in RA production, defects of heart looping (2, 3), reduced posterior chamber (atria and sinus venosus) outgrowth, and defective ventricular trabeculation (4).

RA has been implicated in the early specification and patterning of the cardiac field in zebrafish and avian embryos (5, 6). In the gastrulating chicken embryo, *Raldh2* is first expressed by mesodermal cells posterior to Hensen's node, coinciding with a critical period for anterior–posterior specification of cardiac precursor cells (7). Fate mapping in chicks has shown that *Raldh2*-expressing cells in the lateral mesoderm reside in the proximity of sinoatrial precursors, allowing the diffusion of RA into the cardiac field. Treatment with RA receptor antagonists alters the cardiac fate map and leads to the abnormal presence of ventricular precursors in the posterior cardiac field (7, 8). Further supporting the idea that endogenous RA acts as a regionally restricted signal imparting a sinoatrial fate to cardiac precursor cells, both dietary vitamin A-deficient quail embryos and *Raldh2*$^{-/-}$ knockout mice display abnormal hearts, with a highly hypoplastic inflow tract region and reduced *Tbx5* and *Gata4* expression (4, 6).

Recent findings have changed our view of the origin of cardiac progenitor cells in the mouse embryo. Indeed, several studies have demonstrated that myocytes of the early heart tube derive from two distinct progenitor populations (reviewed in ref. 9). The heart tube is derived from cells of the first heart field (FHF), which begins differentiation at an early stage and mainly contributes to the left ventricle, and in part to the right ventricle and atria. The second heart field (SHF) is a population of undifferentiated multipotent cardiac precursor cells originating from the pharyngeal mesoderm, which first lie medial to the FHF (9). When the FHF differentiates as myocardium, the SHF is left in the forming coelomic or pericardial cavity and lies ventral to the foregut. It is from this position that SHF cells proliferate and are progressively added to the poles of the heart tube (10, 11). The SHF provides the precursor cells of the outflow tract (OFT) and also participates in the formation of the right ventricle and atria (10, 12). Growing evidence suggests the primary site of action of RA may not be in the FHF but in the SHF. Both the *Raldh2*$^{-/-}$ mutants rescued from early lethality by RA supplementation (13) and a hypomorphic *Raldh2* mutant (14) exhibit abnormalities of the OFT and large vessels, reminiscent of the human DiGeorge syndrome and similar to the phenotypes of murine gene knockouts affecting the SHF, including an *Fgf8* hypomorphic and *Tbx1*- and *Foxh1*-null mutations (reviewed in refs. 9 and 15). In later-stage RA-deficiency mutants, OFT defects are accompanied by a profound disorganization of the posterior pharyngeal region and reduced endodermal and mesodermal expression of *Fgf8*, *Hoxa1*, and *Hoxb1* (13, 14).

Here, we used several approaches to examine the contribution of the SHF to pharyngeal mesoderm, atria, and OFT in RA-deficient mouse embryos. By using the *Mlc1v-nlacZ-24* reporter line, in which a *lacZ* transgene has been inserted upstream of the *Fgf10* gene (16), we show that the anterior part of the SHF is disorganized and posteriorly expanded in *Raldh2*$^{-/-}$ mutants, beginning at the four- to five-somite (forming heart tube) stage. The endogenous patterns of *Tbx1* and *Fgf8* expression confirm

Author contributions: L.R. and Z.W. contributed equally to this work; S.Z. and K.N. contributed equally as senior authors; L.R., S.Z., and K.N. designed research; L.R., Z.W., N.B., S.-C.L., X.C., S.Z., and K.N. performed research; X.C. and R.S. contributed new reagents/analytic tools; L.R., S.Z., and K.N. analyzed data; and L.R., S.Z., and K.N. wrote the paper.

The authors declare no conflict of interest.

§To whom correspondence may be addressed. E-mail: zaffran@ibdml.univ-mrs.fr or karenn@bcm.tmc.edu.

This article contains supporting information online at www.pnas.org/cgi/content/full/0712344105/DC1.

© 2008 by The National Academy of Sciences of the USA

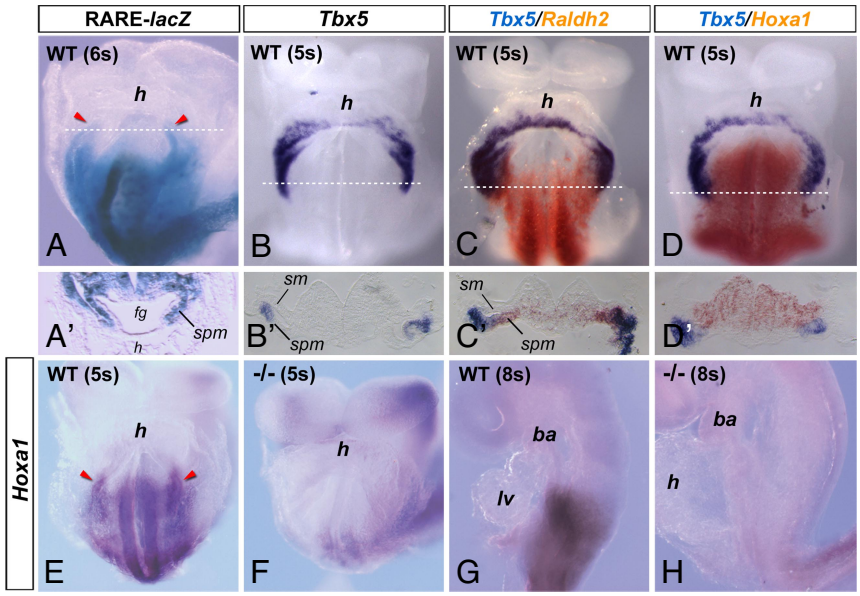

Fig. 1. Retinoid signaling in the early mouse heart. (*A–D*) Ventral views of WT embryos at the five- to six-somite stage (5–6s). (*A′–D′*) Cryosections of the embryos shown in *A–D*, with dotted lines indicating planes of sections. (*A* and *A′*) WT *RARE-hsp68-lacZ* transgenic embryo at six-somite stage exhibits a domain of retinoid activity in the splanchnic mesoderm (spm) adjacent to the forming heart tube (*A*, arrowheads). (*B* and *B′*) Whole-mount ISH of *Tbx5* in a five-somite-stage WT embryo shows robust expression in the posterior most heart portion. (*C* and *C′*) Double ISH of *Tbx5* and *Raldh2* in a five-somite-stage WT embryo reveals complementary, although partly overlapping, expression domains in the splanchnic mesoderm. (*D* and *D′*) Double ISH of *Tbx5* and *Hoxa1* in a five-somite-stage WT embryo shows adjacent expression domains in splanchnic mesoderm. Whole-mount ISH of *Hoxa1* in WT (*E* and *G*) and *Raldh2*$^{-/-}$ (*F* and *H*) embryos indicates that RA is required to induce *Hoxa1* expression adjacent to the cardiac field (*E* and *F*) and caudal pharyngeal field (*G* and *H*). The arrowheads (*E*) indicate expression nearest to the cardiac field. ba, first branchial arch; fg, foregut; h, forming heart tube; lv, left ventricle; sm, somatic mesoderm; spm, splanchnic mesoderm.

this caudal expansion also seen with *Islet-1* (*Isl1*), which marks the whole SHF. Explant studies indicated that the differentiation of cardiac progenitor cells located in the SHF is compromised under *Raldh2* deficiency, likely because of alterations in growth factor signaling. In mutant embryos, the OFT, which derives from the SHF, is absent and there is a severe disorganization of the inflow tract. By using additional *lacZ* reporter transgenic lines, we show that the RA-deficient heart tube is mainly formed of myocardial cells with a right and left ventricular identity, suggesting that the FHF contribution is not altered. Altogether, these results document a role of RA in regulating SHF dynamics.

In the zebrafish embryo, RA deficiency leads to an enlargement of the early domains of *Nkx2.5* expression, suggesting that RA restricts the allocation of cardiac progenitors in the forming cardiac field (5). Here, we provide evidence that the regulation of *Nkx2.5* by RA signaling may be direct, because we found that the upstream regulatory region of the murine *Nkx2.5* gene contains five evolutionarily conserved RA-response elements of the direct-repeat 5′ (DR5) type, which may control late aspects of *Nkx2.5* regulation in SHF-derived OFT cells. To further examine *Raldh2-Nkx2.5* cross-regulation, we generated double mutant mice and found that *Nkx2.5* haploinsufficiency partly rescues the posterior–anterior gradient of *Tbx5* expression in the heart tube of *Raldh2*$^{-/-}$ mutants.

Results

To assess retinoid activity in the WT cardiac field, we used mice harboring the *RARE-hsp68-lacZ* transgene, a sensitive reporter for endogenous RA activity (17). This transgene has been shown to be expressed in the posterior region of the early heart (8), and we confirmed that expression was localized to two dorsal–medial streams of the forming heart tube (Fig. 1*A*, arrowheads), a domain absent in *Raldh2*$^{-/-}$ mutants (data not shown). At the five-somite stage, *Raldh2* and *Tbx5* expression domains converged to overlap in the most posterior cardiac precursors in the splanchnic mesoderm (Fig. 1 *B* and *C*). Similar domains of the RA-responsive *Hoxa1* homeobox gene (18) were present adjacent to the cardiac field in WT embryos at the five- to eight-somite stages (Fig. 1 *D*, *E*, and *G*), but these domains were absent in *Raldh2*$^{-/-}$ embryos (Fig. 1 *F* and *H*).

We crossed *Raldh2*$^{+/-}$ mice with the *Mlc1v-nlacZ-24* line, in which a transgene integration into the *Fgf10* locus leads to transgene expression in the cardiac progenitors located in the anterior heart field and, because of perduration of β-galactosidase (β-gal), activity allows for marking the corresponding myocardial derivatives (16). Although the early expression of this reporter transgene did not show a major difference between WT and *Raldh2*$^{-/-}$ mutants at the one- to two-somite stages (Fig. 2 *A* and *B*), from the five-somite stage, its expression was clearly altered in mutants. First, the labeled cells were dramatically expanded toward posterior regions (compare Fig. 2 *C* and *D*, arrowheads), an alteration that was accentuated at the seven-somite stage (Fig. 2 *E–J′*). Thus, in *Raldh2*$^{-/-}$ mutants the X-gal staining was present in the lateral mesoderm well beyond the level of the developing heart tube (compare Fig. 2 *I′* with *J′*, arrowheads). Second, the closure of the dorsal mesocardium was defective, because the midline gap in X-gal staining became progressively wider in the *Raldh2*$^{-/-}$ mutants (Fig. 2 *D*, *F*, and *J*, brackets). To examine the activation of the *Mlc1v-nlacZ-24* transgene in the lateral mesoderm lying posterior to the heart tube, explants from this region were dissected at the zero- to two-somite stage (a stage at which the transgene is not activated posteriorly in *Raldh2*$^{-/-}$ embryos; Fig. 2 *A* and *B*) and cultured for 36 h. Explants from *Raldh2*$^{-/-}$ mutants were X-gal-positive after the *in vitro* culture (data not shown), indicating that the expanded *Mlc1v-nlacZ-24* pattern observed in whole embryos does not result from an abnormal migration of anterior cells. At later stages [embryonic day (E)9.0], X-gal activity in *Mlc1v-nlacZ-24*;*Raldh2*$^{-/-}$ mutants was spatially reduced compared with control embryos (Fig. 2 *K* and *L*). The staining adjacent to

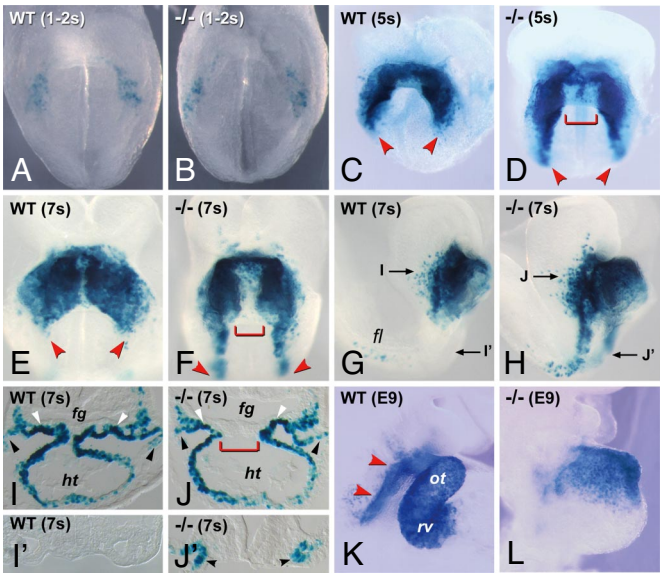

Fig. 2. Retinoid deficiency causes SHF defects. WT and *Raldh2*$^{-/-}$ *Mlc1V-nlacZ-24* transgenic embryos were analyzed by X-gal staining (*A–F*, ventral views; *G*, *H*, *K*, and *L*, right-side views; *I–J′*, transverse sections). At the one- to two-somite stage, transgene expression is unaltered in mutants (*A* and *B*). At the five-somite (*C* and *D*) and seven-somite (*E* and *F*) stages, red arrowheads point to the caudal limit of expression in the SHF, which is expanded in *Raldh2*$^{-/-}$ mutant embryos (*D* and *F*). Note the abnormally large gap in midline staining in mutants (brackets). (*G* and *H*) Right-side views of embryos shown in *E* and *F*. The arrows indicate planes of sections in *I–J′*. (*I* and *J*) Transverse sections reveal β-gal^{+} cells in splanchnic epithelium (white arrowheads) adjacent to foregut endoderm, in somatic mesoderm (black arrowheads), and in heart tube myocardium. Note that dorsal mesocardium is not closed in the *Raldh2*$^{-/-}$ embryo (*J*, bracket). (*I′* and *J′*) Expansion of *Mlc1v-nlacZ-24* transgene expression is seen in posterior lateral mesoderm (arrowheads) of the *Raldh2*$^{-/-}$ mutant (*J′*). (*K* and *L*) Right-side views of E9.0 WT and *Raldh2*$^{-/-}$ embryos, showing details of the heart and adjacent pharyngeal region. The arrowheads point to pharyngeal staining, which is almost undetectable in the mutant. fl, forelimb; ht, heart tube; ot, OFT; rv, right ventricle.

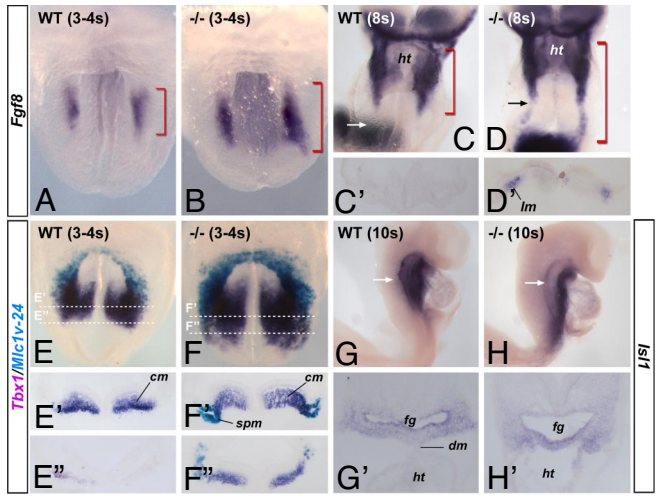

Fig. 3. Caudal expansion of the SHF in RA-deficient mutants. Whole-mount ISH analysis of *Fgf8* (*A–D′*), *Tbx1* combined with X-gal staining for *Mlc1v-nlacZ-24* (*E–F″*) and *Isl1* (*G–H′*). The arrows or dotted lines in *C–H* indicate planes of sections shown in *C′–H′*. (*A–D*) Brackets indicate endogenous *Fgf8* expression in the anterior part of the SHF, which is expanded in *Raldh2*$^{-/-}$ mutants (*B* and *D*). (*D′*) A transverse section of the embryo shown in *D* reveals *Fgf8* expression in the lateral mesoderm. (*E* and *F*) Ventral of WT and *Raldh2*$^{-/-}$ embryos at the three- to four-somite stage showing a caudal expansion of *Mlc1v-nlacZ-24* transgene expression and *Tbx1*. (*E′–F″*) Transverse sections further illustrate the caudal expansion of *Mlc1v-nlacZ-24* transgene activity and *Tbx1* transcripts. (*G* and *H*) Right-side views of WT and *Raldh2*$^{-/-}$ embryos at the 10-somite stage showing an expansion of the pan-SHF marker *Isl1* under RA deficiency (*H*). (*G′* and *H′*) Transverse sections show *Isl1* expression in the splanchnic mesoderm (the SHF) and the ventral foregut endoderm of both embryos. Of note, there is no ectopic expression of *Isl1* transcripts in the myocardium of the mutant heart (compare *G′* with *H′*). cm, cranial mesoderm; dm, dorsal mesocardium; lm, lateral mesoderm.

the WT second and third pharyngeal arches (Fig. 2*K*, arrowheads) was absent in mutants, although expression was detected in the anterior portion of the "unlooped" heart tube (Fig. 2 *K* and *L*).

We examined expression of other anterior markers of the SHF such as *Fgf8* and *Tbx1*. *Fgf8* expression was more intense and caudally expanded in *Raldh2*$^{-/-}$ mutants, from the three- to four-somite stage onward (Fig. 3 *A–D*). As for the *Mlc1v-nlacZ-24* transgene, *Fgf8* expression was detected in the posterior lateral mesoderm of the *Raldh2*$^{-/-}$ mutant embryos at the eight-somite stage (Fig. 3 *C′* and *D′*; the greater expansion of the *Mlc1v-nlacZ-24* transgene may be attributable to β-gal stability). The T-box gene *Tbx1*, frequently deleted in human 22q11 deletion DiGeorge syndrome (reviewed in ref. 15), appears to be genetically upstream of *Fgf8* (19–22). WT embryos exhibited pronounced *Tbx1* expression in the SHF region caudal–medial to *Mlc1v-nlacZ-24* reporter staining (Fig. 3 *E* and *E′*), whereas *Tbx1* expression appeared more intense and expanded in range in *Raldh2*$^{-/-}$ mutants starting at the three- to four-somite stage (Fig. 3 *F* and *F′* and data not shown). We also examined expression of a pan-SHF progenitor cell marker, *Isl1* (10). *Isl1*-expressing cells in the splanchnic mesoderm give rise to cardiomyocytes of the OFT, the right ventricle, atria, and inflow region of the heart (10). *Isl1* is also expressed in ventral and lateral foregut endoderm (see Fig. 3*G′*). Caudal expansion of *Isl1* expression was observed in *Raldh2*$^{-/-}$ mutants (Fig. 3 *G* and *H*), but the labeled cells did not extend into the heart tube where cardiomyocytes are present (Fig. 3 *G′* and *H′*). Altogether, these observations suggest that endogenous RA may control the antero-posterior location of cardiac progenitors of the SHF within the splanchnic mesoderm.

Excess RA levels can often affect the same RA-regulated signaling pathways as RA deficiency but in an opposite manner. This was found to be the case when a single dose of RA was administered to WT mice at late gastrulation (E7.5). These treatments resulted in marked reductions of endogenous *Fgf8* and *Isl1* transcripts and of *Mlc1v-nlacZ-24* reporter transgene staining [supporting information (SI) Fig. 6].

We then examined *Raldh2*$^{-/-}$ mutants for endogenous expression of *Bmp2*, *-4*, *-6* and *-7*, which encode TGFβ family members influencing myocardial differentiation (reviewed in ref. 23). We found *Bmp6*, *Bmp7* (SI Fig. 7 *A–D*), and *Bmp2* (see Fig. 5 *F* and *H*) levels to be reduced in the inflow region of the mutants. Interestingly, at later stages (E9.0), *Tgfβ2* expression was markedly increased at the venous pole (septum transversum) of the *Raldh2*$^{-/-}$ unlooped heart (SI Fig. 7 *E* and *F*). A similar hyperactivation of TGFβ signaling is observed in foregut tissues of *Raldh2*$^{-/-}$ mutants at E8.5 and has been implicated in the lack of lung induction (24).

The reductions in levels of *Mlc1v-nlacZ-24* transgene expression (an *Fgf10* enhancer trap) in the pharyngeal mesoderm of *Raldh2*$^{-/-}$ mutants at E9 (Fig. 2 *K* and *L*) suggest that FGF signaling may be affected in the SHF. To further investigate this pathway, we performed immunolocalization of p-ERK1/2, effectors of MAP signaling whose phosphorylation correlates with FGF activity in the cardiac region (25). p-ERK1/2 levels were found to be lower in the SHF at the 10-somite stage in *Raldh2*$^{-/-}$ embryos (SI Fig. 7 *G* and *H*). Consistent with the decrease of *p*-ERK levels, the expression of other FGF downstream targets

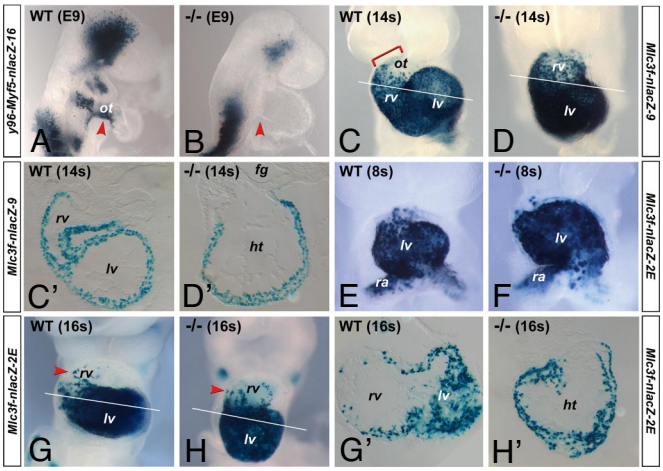

Fig. 4. Transgenic reporter lines reveal OFT defects and normal FHF contribution in *Raldh2*$^{-/-}$ embryos. (*A* and *B*) Right-side views of X-gal stained E9 WT and *Raldh2*$^{-/-}$ embryos, showing absence of *y96-Myf5-nlacZ-16* transgene expression, a marker of the OFT (arrowheads), in the mutant. (*C* and *D*) In *Mlc3f-nlacZ-9* hearts at the 14-somite stage, X-gal staining distinguishes the OFT lacking transgene activity (*C*, bracket) and the right ventricle. β-Gal activity is also detected in the left ventricle. The nonexpressing domain (presumptive OFT) is absent under RA deficiency (*D*). The white lines indicate planes of sections in *C*′ and *D*′. (*E* and *F*) At the eight-somite stage, *Mlc3f-nlacZ-2E* transgene expression marks the presumptive right atria and left ventricle in both WT (*E*) and *Raldh2*$^{-/-}$ mutants (*F*). (*G* and *H*) Ventral views of X-gal stained *Mlc3f-nlacZ-2E* WT and *Raldh2*$^{-/-}$ embryos at the 16-somite stage showing the distinction between right (arrowheads) and left ventricles. White lines indicate planes of sections in *G*′ and *H*′. ra, right atria.

(*Sprouty1* and *-2* and *Mkp3*; SI Fig. 7 *I–J*′ and data not shown) was also reduced in the pharyngeal region and splanchnic mesoderm of mutants.

To examine myocardial subdomains in the RA-deficient hearts, we crossed *Raldh2*$^{+/-}$ mutants with additional, region-specific reporter transgenes. The *y96-Myf5-nlacZ-16* transgene displays a domain of expression in the WT OFT myocardium beginning at the 12- to 14-somite stage (26), which was absent in *Raldh2*$^{-/-}$ mutants (Fig. 4 *A* and *B*). The absence or reduction of OFT myocardium in mutants was confirmed by the *Mlc3f-nlacZ-9* pattern (Fig. 4 *C* and *D*). This transgene is known to be silenced in WT OFT myocardium (12) (Fig. 4*C*, bracket). In mutants, most if not all of the unlooped heart tube contained *Mlc3f-nlacZ-9*-labeled cells (Fig. 4*D*). These observations indicate that the deployment of SHF cells to the OFT was highly compromised in *Raldh2*$^{-/-}$ mutant embryos. In contrast, the activity of the *Mlc3f-nlacZ-2E* transgene, normally expressed in left but not right ventricular myocardium (Fig. 4 *E* and *G*), was well detected in the *Raldh2*$^{-/-}$ heart tube (compare Fig. 4 *E* and *G* with *F* and *H*) (12). These results strongly suggest that FHF contribution is not affected under RA deficiency. To estimate the myocardial cell numbers and the presence of differentiating cardiomyocytes in the *Raldh2*$^{-/-}$ mutant hearts, we counted the number of β-gal-positive and α-actinin-positive cells on serial sections of WT and *Raldh2*$^{-/-}$ embryos from the *Mlc3f-nlacZ-9* line (SI Fig. 8). At E9.5, we estimated a deficiency of ≈30%, both in the overall number of β-gal-positive cells and of differentiating (α-actinin-positive) cardiomyocytes in *Raldh2*$^{-/-}$ mutants, which may correspond to the defects observed in the outflow and inflow regions.

To further explore the differentiation potential of *Raldh2*$^{-/-}$ cardiomyocytes, explants of SHF isolated from three- to five-somite stage WT and *Raldh2*$^{-/-}$ embryos carrying the *Mlc1v-nlacZ-24* transgene were cultured for 48 h and X-gal-stained to identify SHF cells and derivatives (12, 16). Under these established culture conditions, WT SHF explants consistently underwent cardiac differentiation, characterized by the presence of beating cells and expression of myosin heavy chain (MF20), quite similar to heart explants cultured from the same embryos (SI Table 1; also see ref. 12). *Raldh2*$^{-/-}$ mutant SHF explants, however, never differentiated or formed beating cardiomyocytes, in contrast to their heart, which was still beating under the same culture conditions (SI Table 1). This suggested that the *Raldh2*$^{-/-}$ mutant SHF was impaired in its ability to contribute to differentiated cardiomyocytes, potentially because of reduced bone morphogenetic protein (BMP) signaling.

The intriguing finding that both *Raldh2* deficiency and RA receptor antagonism in zebrafish embryos resulted in the production of excess myocardial progenitors, marked by up-regulated *Nkx2.5* expression during gastrulation (5), led us to investigate potential mechanisms for cross-regulation between the retinoid and Nkx2.5 transcriptional pathways. One avenue to examine such interactions is to generate compound mutants. Insertion of a Cre transgene in the *Nkx2.5* locus (27) disrupts expression of this gene, so that when mated to homozygosity, the resulting embryos phenocopy previously reported *Nkx2.5*$^{-/-}$ mutants (27–29). We crossed *Nkx2.5*-Cre mutants with *Raldh2*$^{+/-}$ mice and analyzed compound mutants at E8.5 for *Tbx5* expression as a marker for the posterior portion of the heart, which is destined to become the sinus venosa and atria (30). As expected, the domain of *Tbx5* expression was reduced in *Raldh2*$^{-/-}$ embryos (compare Fig. 5 *A* with *C*), correlating with an abnormal morphogenesis of the inflow region (4). Interestingly, *Nkx2.5* haploinsufficiency partially rescued *Tbx5* expression in *Raldh2*$^{-/-}$ embryos (Fig. 5*D*). Complete *Nkx2.5* deficiency further expanded *Tbx5* expression in *Raldh2*$^{-/-}$; *Nkx2.5*$^{-/-}$ compound mutants (Fig. 5*E*). Prall *et al.* (31) have demonstrated that *Nkx2.5* deficiency up-regulates *Bmp2* expression, which may result in increased myocardial differentiation. We likewise observed expanded *Bmp2* expression in our *Nkx2.5*$^{-/-}$ mutants (Fig. 5*G*). Although *Bmp2* levels were reduced in *Raldh2*$^{-/-}$ mutants (Fig. 5*H*), we found that these levels were progressively normalized upon removal of functional *Nkx2.5* alleles (Fig. 5 *I* and *J*). Additionally, SHF expression, as assayed by *Isl1* expression, appeared essentially unaltered in *Raldh2*$^{-/-}$ mutants under *Nkx2.5* deficiency (data not shown).

By performing a VISTA-based promoter search for transcriptional binding sites in evolutionary conserved regions, we uncovered an upstream regulatory region of the *Nkx2.5* gene containing five conserved RA-response elements (RAREs) of the DR5 type. A *lacZ* transgenic line was generated by using a BAC fragment containing the region located from −14.8 to −7.5 kb upstream of the *Nkx2.5* transcriptional start site, which included the RAREs. This fragment was sufficient to drive *lacZ* reporter expression in the FHF (SI Fig. 9 *A–C*), similar to endogenous *Nkx2.5* expression (28). Whereas the early domain of endogenous *Nkx2.5* (data not shown) and *Nkx2.5* transgene expression in the cardiac crescent was not altered in *Raldh2*$^{-/-}$ mutants (SI Fig. 9 *D–F*), endogenous *Nkx2.5* was expanded in the SHF of mutants at E8.5 (SI Fig. 9 *G* and *H*, arrowheads). However, transgene expression was reduced in the OFT and the right ventricle of RA-supplemented *Raldh2*$^{-/-}$ embryos at E10.5 (SI Fig. 9 *I* and *J*). These observations suggest that *Nkx2.5* regulation is not RA-dependent in the FHF and at early stages in the SHF, although eventually it is affected when RA levels are decreased at later stages of development.

Discussion

Originally RA was proposed to regulate the anterior–posterior specification of cardiac progenitors within the FHF. Indeed, posterior cells of the early FHF are encircled by *Raldh2*-expressing cells in the lateral mesoderm. Blocking RA signaling in chick embryos inhibited atrial differentiation and altered the cardiac fate map, so that ventricular progenitors extended outside of their normal

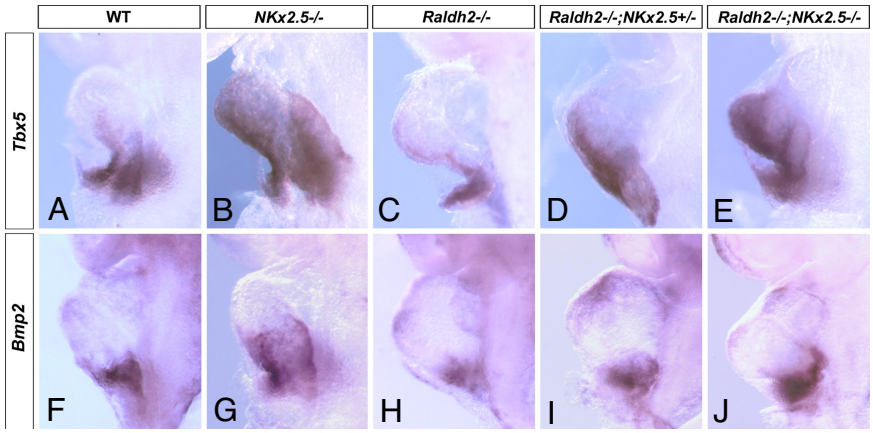

Fig. 5. Genetic interaction between the retinoid and Nkx2.5 pathways. Sinoatrial *Tbx5* expression (*A*, WT embryo) is reduced in *Raldh2*$^{-/-}$ mutants (*C*). Inactivation of one *Nkx2.5* allele results in an expanded *Tbx5* domain in *Raldh2*$^{-/-}$ mutants (*D*), similar to *Nkx2.5*$^{-/-}$ mutants (*B*) and *Nkx2.5*$^{-/-}$;*Raldh2*$^{-/-}$ double mutants (*E*). *Bmp2* expression (*F*, WT embryo) is increased in *Nkx2.5*$^{-/-}$ mutants (*G*) and moderately reduced in *Raldh2*$^{-/-}$ mutants (*H*). Inactivation of one (*I*) or both (*J*) *Nkx2.5* allele(s) progressively increases *Bmp2* levels in *Raldh2*$^{-/-}$ mutants. All embryos are at the 8- to 10-somite stage. Profile views are shown.

domains (7). Keegan *et al.* (5) further have found that RA deficiency results in an expansion of cardiac progenitors during gastrulation in zebrafish, via a direct fate transformation.

Our results, although partly consistent with previous findings, now show that RA regulates SHF organization within the precise time frame in which RA deficiency affects cardiac formation in avian and mammalian models. We also observed an overlap between the region of RA signaling and the caudal limit of SHF marker gene expression, correlating with an anterior domain of *Hoxa1* expression in WT embryos, a domain that is absent in *Raldh2* mutants. Because restoring *Hoxa1* expression in RA-deficient amphioxus embryos can rescue patterning defects (32), we postulate that the lack of *Hoxa1* expression in the cardiac field may result in cardiac perturbations found in *Raldh2* mutants (4). We found that the earliest events of cardiac RA deficiency were the caudal expansions of SHF gene expression, occurring at a stage when cardiac defects become irreversible in an avian vitamin A-deficiency model (33). We propose that these initial molecular alterations in SHF expression are why RA-deficient heart formation cannot be restored after this time. Additional reductions in the right ventricle and absence of OFT because of impaired SHF integration in the forming heart tube probably contributes to abnormal cardiac looping also found in other SHF mutants such as *Isl1*, *Mef2c*, and *Nkx2.5* (10, 31, 34).

Some genetic cross-talk exists between Nkx2.5 and RA signaling, because we show here that reducing *Nkx2.5* gene dosage can rescue aspects of the *Raldh2*$^{-/-}$ cardiac phenotype, including *Tbx5* expression. *Nkx2.5*$^{-/-}$ mutants have an apparent expansion of the FHF contribution to the left ventricle (31). Hence it may have been expected that *Nkx2.5* loss of function would have worsened the *Raldh2*$^{-/-}$ cardiac phenotype. More likely it is the feedback repression that Nkx2.5 normally imposes on Bmp2/Smad signaling (31), which when relieved may improve the RA deficiency phenotype. Transplantation of WT foregut endoderm, or exogenous supply of BMP2 and Gata4, can restore heart morphology in vitamin A-deficient quail embryos (35, 36). Although *Bmp2* expression indeed appears up-regulated in *Nkx2.5*;*Raldh2* compound mutants, further genetic strategies are required to clarify the precise manner by which these two signaling pathways interact.

The importance of *Fgf8* in SHF signaling has been noted (19, 20, 22, 37, 38). Our study indicates that a primary mechanism by which RA regulates SHF dynamics may be by modulating FGF signaling. We show that endogenous RA is required to prevent *Fgf* expression in the posterior lateral mesoderm (including in the posterior region of the SHF). Not only did RA deficiency lead to expanded *Fgf8* and *Fgf10* (*Mlc1v-nlacZ-24*-enhancer trap) expression, this expansion occurred at approximately the five-somite stage, when cardiac defects become irreversible in the quail vitamin A-deficiency model (33). Conversely, we saw that excess exogenous RA reduces SHF *Fgf8* levels, similar to what has been observed when endogenous RA is increased by blocking the activity of its metabolizing CYP26 enzymes (39).

One puzzling finding in *Raldh2* mutants was that despite the expansion of the SHF at early stages of development, eventually the contribution of SHF cells to the heart tube was compromised. Explant studies demonstrate that mutant SHF cells are impaired in their ability to differentiate and to form beating cardiomyocytes. Several explanations may account for these findings. Reduction in BMP signaling, found in *Raldh2* mutants, may lead to the absence of bona fide cardiac induction. Accordingly, FGFs can only elicit cardiomyogenic effects in regions where BMP signaling is also present (40). Alternately, the expanded early FGF8 signaling may hinder the capacity of the prospective myocardial SHF cells to develop and correctly function, similar to what is observed at slightly later stages when excess FGF8 resulting from cardiac neural crest ablation disrupts myocardial function (37, 41). Moreover, altering RA-*Fgf8* regulatory interactions may produce adverse consequences. In prostate cancer cells, RA activation of the *Fgf8* promoter produces a switch of splice isoforms, so that a less mitotically active isoform (*Fgf8a*) accumulates (42). Because both canonical and novel RA-response elements in the *Fgf8* promoter can be activated by unliganded RARα in COS cells (43), an absence of RA may produce an accumulation of the more proliferative *Fgf8b* product. Hypothetically, the absence of RAR ligand in *Raldh2*$^{-/-}$ mutants may favor *Fgf8b* expression, hindering early SHF progenitor differentiation by its increased mitotic activity.

In conclusion, mutual inhibition between FGF and RA pathways may control cardiac stem cell dynamics and cardiomyocyte differentiation, similar to what has been described during caudal neuronal stem cell production and neural tube differentiation (reviewed in ref. 44). In this tail bud of chick embryos at early somite stages, *Fgf8* expression marks the caudal source of neuronal stem cells, which under RA deficiency is expanded. The ability of neural progenitors to differentiate, however, is impaired when RAR signaling is blocked (44). Similarly we observed that cardiac stem cell populations, marked by *Isl1* expression (45), were expanded under RA deficiency, whereas SHF cardiomyocyte differentiation was impaired. Further un-

derstanding of how RA regulates cardiac progenitors and growth factor pathways in the early embryo may engender novel ideas about how to regulate cardiac stem cell dynamics in humans.

Materials and Methods

***In Situ* Hybridization and Immunohistochemistry.** *Raldh2*-null mutant mice have been described (3) as well as the maternal RA supplementation procedure (46). The *lacZ* reporter transgenic lines have been described (12, 26). Whole-mount *in situ* hybridization (ISH) was performed as described (12) by using Intavis InSituPro robots. Double whole-mount ISH with digoxigenin- and FITC-labeled riboprobes were performed according to the Stern laboratory protocol. Transgenic expression was monitored by X-gal assays as described (12). Whole-mount immunolabeling with anti p-ERK1/2 antibody (Cell Signaling) was performed according to the Rossant laboratory protocol.

Retinoic Acid Treatment of Embryos. All-*trans*-RA (Sigma) was dissolved in DMSO and diluted at 20 mg/ml. At E7.5, the mice were given a single i.p. injection of the RA solution (65 mg/kg) or control DMSO.

Embryonic Explant Cultures. The region posterior to the FHF up to the allantois was dissected from zero- to two-somite stage embryos collected and transferred to culture medium in collagen (1%) coated multiwell dishes. For older embryos, the heart tube alone or pharyngeal mesoderm (including pharyngeal endoderm) was dissected and transferred to culture medium. Explants were cultured as described (12) for 36 to 48 h. Fluorescent immunohistochemistry was performed by using the anti-myosin heavy chain antibody MF20 (Developmental Studies Hybridoma Bank, University of Iowa, Iowa City, IA) at a 1/100 dilution. Explant experiments were repeated several times for each transgenic line and time point (SI Table 1).

Analysis of Myocardial Cell Numbers. Cell counting was assessed on 14-μm sections by using rabbit polyclonal anti-β-Gal (1:500; Cappel) and monoclonal anti-sarcomeric α-actinin (clone EA-53, 1:500; Sigma) followed by DAPI staining. The number of myocardial cells (DAPI$^+$ nuclei in α-actinin$^+$ cells) and β-gal$^+$ cells (combined DAPI$^+$ and β-Gal$^+$ nuclei) were recorded on all serial sections of *Mlc3f-nlacZ-9* transgenic embryos ($n = 3$ for each genotype) at E9.5.

ACKNOWLEDGMENTS. We thank Dr. J. Rossant (Hospital for Sick Children, Toronto) for providing RARE-hsp68-*lacZ* mice; Drs. M. Buckingham (Pasteur Institute, Paris) and R. Kelly (Developmental Biology Institute, Marseille) for providing the *y96-Myf5-nlacZ-16*, *Mlc3f-nlacZ-9*, *Mlc3f-nlacZ-2E*, and *Mlc1v-nlacZ-24* transgenic mice; Drs. P. Chambon (Institut de Génétique et de Biologie Moléculaire et Cellulaire, Illkirch, France), V. Christoffels (Heart Failure Research Center, Amsterdam), D. Duboule (National Research Centre, Lausanne), B. Hogan (Duke University, Durham, NC), R. Kelly, C. C. Hui (Hospital for Sick Children, Toronto), G. Martin (University of California, San Francisco), A. McMahon (Harvard University, Cambridge, MA), and E. Olson (University of Texas Southwestern Medical Center, Dallas) for template plasmids; and Drs. M. Buckingham and P. Dollé for advice throughout the study and comments on the manuscript. This work was supported by National Institutes of Health Grant R01 HL070733 and American Heart Association Grant 0330265N (to K.N.), the Centre National de la Recherche Scientifique (S.Z.), and Association Française Contre les Myopathies Grant AFM 12495 (to S.Z.). L.R. received fellowships from the Ministère de la Recherche and the Université d'Aix-Marseille II (Monitorat).

1. Niederreither K, Dolle P (2008) Retinoids and heart development. *Heart Development*, eds Rosenthal N, Harvey RP (Academic, San Diego).
2. Mic FA, Haselbeck RJ, Cuenca AE, Duester G (2002) Novel retinoic acid generating activities in the neural tube and heart identified by conditional rescue of Raldh2 null mutant mice. *Development* 129:2271–2282.
3. Niederreither K, Subbarayan V, Dolle P, Chambon P (1999) Embryonic retinoic acid synthesis is essential for early mouse post-implantation development. *Nat Genet* 21:444–448.
4. Niederreither K, *et al.* (2001) Embryonic retinoic acid synthesis is essential for heart morphogenesis in the mouse. *Development* 128:1019–1031.
5. Keegan BR, Feldman JL, Begemann G, Ingham PW, Yelon D (2005) Retinoic acid signaling restricts the cardiac progenitor pool. *Science* 307:247–249.
6. Kostetskii I, *et al.* (1999) Retinoid signaling required for normal heart development regulates GATA-4 in a pathway distinct from cardiomyocyte differentiation. *Dev Biol* 206:206–218.
7. Hochgreb T, *et al.* (2003) A caudorostral wave of RALDH2 conveys anteroposterior information to the cardiac field. *Development* 130:5363–5374.
8. Moss JB, *et al.* (1998) Dynamic patterns of retinoic acid synthesis and response in the developing mammalian heart. *Dev Biol* 199:55–71.
9. Buckingham M, Meilhac S, Zaffran S (2005) Building the mammalian heart from two sources of myocardial cells. *Nat Rev Genet* 6:826–835.
10. Cai CL, *et al.* (2003) Isl1 identifies a cardiac progenitor population that proliferates prior to differentiation and contributes a majority of cells to the heart. *Dev Cell* 5:877–889.
11. Meilhac SM, Esner M, Kelly RG, Nicolas JF, Buckingham ME (2004) The clonal origin of myocardial cells in different regions of the embryonic mouse heart. *Dev Cell* 6:685–698.
12. Zaffran S, Kelly RG, Meilhac SM, Buckingham ME, Brown NA (2004) Right ventricular myocardium derives from the anterior heart field. *Circ Res* 95:261–268.
13. Niederreither K, *et al.* (2003) The regional pattern of retinoic acid synthesis by RALDH2 is essential for the development of posterior pharyngeal arches and the enteric nervous system. *Development* 130:2525–2534.
14. Vermot J, Niederreither K, Garnier JM, Chambon P, Dolle P (2003) Decreased embryonic retinoic acid synthesis results in a DiGeorge syndrome phenotype in newborn mice. *Proc Natl Acad Sci USA* 100:1763–1768.
15. Baldini A (2004) DiGeorge syndrome: An update. *Curr Opin Cardiol* 19:201–204.
16. Kelly RG, Brown NA, Buckingham ME (2001) The arterial pole of the mouse heart forms from Fgf10-expressing cells in pharyngeal mesoderm. *Dev Cell* 1:435–440.
17. Rossant J, Zirngibl R, Cado D, Shago M, Giguere V (1991) Expression of a retinoic acid response element-hsplacZ transgene defines specific domains of transcriptional activity during mouse embryogenesis. *Genes Dev* 5:1333–1344.
18. Dupe V, *et al.* (1997) *In vivo* functional analysis of the Hoxa-1 3′ retinoic acid response element (3′RARE). *Development* 124:399–410.
19. Abu-Issa R, Smyth G, Smoak I, Yamamura K, Meyers EN (2002) Fgf8 is required for pharyngeal arch and cardiovascular development in the mouse. *Development* 129:4613–4625.
20. Frank DU, *et al.* (2002) An Fgf8 mouse mutant phenocopies human 22q11 deletion syndrome. *Development* 129:4591–4603.
21. Kochilas L, *et al.* (2002) The role of neural crest during cardiac development in a mouse model of DiGeorge syndrome. *Dev Biol* 251:157–166.
22. Vitelli F, *et al.* (2002) A genetic link between Tbx1 and fibroblast growth factor signaling. *Development* 129:4605–4611.
23. Lough J, Sugi Y (2000) Endoderm and heart development. *Dev Dyn* 217:327–342.
24. Chen F, *et al.* (2007) Inhibition of Tgfb signaling by endogenous retinoic acid is essential for primary lung bud induction. *Development* 134:2969–2979.
25. Corson LB, Yamanaka Y, Lai KM, Rossant J (2003) Spatial and temporal patterns of ERK signaling during mouse embryogenesis. *Development* 130:4527–4537.
26. Bajolle F, *et al.* (2006) Rotation of the myocardial wall of the outflow tract is implicated in the normal positioning of the great arteries. *Circ Res* 98:421–428.
27. Moses KA, DeMayo F, Braun RM, Reecy JL, Schwartz RJ (2001) Embryonic expression of an Nkx2–5/Cre gene using ROSA26 reporter mice. *Genesis* 31:176–180.
28. Lyons I, *et al.* (1995) Myogenic and morphogenetic defects in the heart tubes of murine embryos lacking the homeo box gene Nkx2–5. *Genes Dev* 9:1654–1666.
29. Tanaka M, Chen Z, Bartunkova S, Yamasaki N, Izumo S (1999) The cardiac homeobox gene Csx/Nkx2.5 lies genetically upstream of multiple genes essential for heart development. *Development* 126:1269–1280.
30. Bruneau BG, *et al.* (1999) Chamber-specific cardiac expression of Tbx5 and heart defects in Holt-Oram syndrome. *Dev Biol* 211:100–108.
31. Prall OW, *et al.* (2007) An Nkx2–5/Bmp2/Smad1 negative feedback loop controls heart progenitor specification and proliferation. *Cell* 128:947–959.
32. Schubert M, *et al.* (2005) Retinoic acid signaling acts via Hox1 to establish the posterior limit of the pharynx in the chordate amphioxus. *Development* 132:61–73.
33. Kostetskii I, *et al.* (1998) Initial retinoid requirement for early avian development coincides with retinoid receptor coexpression in the precardiac fields and induction of normal cardiovascular development. *Dev Dyn* 213:188–198.
34. Verzi MP, McCulley DJ, De Val S, Dodou E, Black BL (2005) The right ventricle, outflow tract, and ventricular septum comprise a restricted expression domain within the secondary/anterior heart field. *Dev Biol* 287:134–145.
35. Ghatpande S, Brand T, Zile M, Evans T (2006) Bmp2 and Gata4 function additively to rescue heart tube development in the absence of retinoids. *Dev Dyn* 235:2030–2039.
36. Ghatpande S, Ghatpande A, Zile M, Evans T (2000) Anterior endoderm is sufficient to rescue foregut apoptosis and heart tube morphogenesis in an embryo lacking retinoic acid. *Dev Biol* 219:59–70.
37. Hutson MR, *et al.* (2006) Cardiac arterial pole alignment is sensitive to FGF8 signaling in the pharynx. *Dev Biol* 295:486–497.
38. Ilagan R, *et al.* (2006) Fgf8 is required for anterior heart field development. *Development* 133:2435–2445.
39. Roberts C, Ivins S, Cook AC, Baldini A, Scambler PJ (2006) Cyp26 genes a1, b1 and c1 are down-regulated in Tbx1 null mice and inhibition of Cyp26 enzyme function produces a phenocopy of DiGeorge Syndrome in the chick. *Hum Mol Genet* 15:3394–3410.
40. Alsan BH, Schultheiss TM (2002) Regulation of avian cardiogenesis by Fgf8 signaling. *Development* 129:1935–1943.
41. Farrell MJ, *et al.* (2001) FGF-8 in the ventral pharynx alters development of myocardial calcium transients after neural crest ablation. *J Clin Invest* 107:1509–1517.
42. Brondani V, Hamy F (2000) Retinoic acid switches differential expression of FGF8 isoforms in LNCaP cells. *Biochem Biophys Res Commun* 272:98–103.
43. Brondani V, Klimkait T, Egly JM, Hamy F (2002) Promoter of FGF8 reveals a unique regulation by unliganded RARalpha. *J Mol Biol* 319:715–728.
44. Diez del Corral R, Storey KG (2004) Opposing FGF, retinoid pathways: A signalling switch that controls differentiation and patterning onset in the extending vertebrate body axis. *BioEssays* 26:857–869.
45. Laugwitz KL, *et al.* (2005) Postnatal isl1+ cardioblasts enter fully differentiated cardiomyocyte lineages. *Nature* 433:647–653.
46. Niederreither K, *et al.* (2002) Genetic evidence that oxidative derivatives of retinoic acid are not involved in retinoid signaling during mouse development. *Nat Genet* 31:84–88.